

Received April 14, 2022, accepted May 11, 2022. Date of publication xxxx 00, 0000, date of current version xxxx 00, 0000.

Digital Object Identifier 10.1109/ACCESS.2022.3175409

Gait Stability Index Built by Kinematic Information Consistent With the Margin of Stability Along the Mediolateral Direction

TOMOYUKI IWASAKI¹, SHOGO OKAMOTO^{1,2}, (Member, IEEE),
YASUHIRO AKIYAMA³, (Member, IEEE),
AND YOJI YAMADA¹, (Member, IEEE)

¹Department of Mechanical Systems, Nagoya University, Nagoya, Aichi 464-0813 Japan

²Department of Computer Sciences, Tokyo Metropolitan University, Hino, Tokyo 191-0065, Japan

³Department of Mechanical Engineering and Robotics, Shinshu University, Ueda, Nagano 386-0018, Japan

Corresponding author: Shogo Okamoto (okamotos@tmu.ac.jp)

This work was supported in part by Ministry of Education, Culture, Sports, Science and Technology (MEXT) KAKENHI under Grant 19K21584.

ABSTRACT Gait stability indices that can be easily measured and computed are required in both clinical and commercial applications. We established a novel gait stability index based on kinematic information that was substantially correlated with the margin of stability (MoS); a popular kinetic stability index. The novel index was computed using the time-series of triaxial velocities from the human body mass center. The partial least squares regression method was extended to time-series data and applied to the velocity series to compute the principal motions. These motions were elementary motions constructing the gait motions, and their magnitudes in each gait motion were correlated with the MoS. Gait data from 60 participants (30 males and 30 females; age: 67.6 ± 3.4 years (mean and standard deviation); height: 159.6 ± 7.6 cm; weight: 60.6 ± 9.3 kg) were analyzed. The combination of three principal motions exhibited a moderate correlation with the minimum MoS values in the mediolateral direction at $r = 0.68$, suggesting that the novel kinematic index can be used as an easy-to-access alternative to the MoS. The established kinematic index can be a substitute for the margin of stability.

INDEX TERMS Gait stability, partial least squares regression, principal motion analysis, margin of stability.

I. INTRODUCTION

To date, gait stability and stable walking have been intensively studied by many researchers. It has been shown that stable gait relies on gait parameters comprising stride length and walking speed [1]–[6]. In particular, gait stability indices are useful in judging the risk of falling [7], [8].

There exist two categories of gait stability indices: kinetic and kinematic. Kinetic indices are computed based on mechanical dynamics and indicate physical resistance towards falls; however, they require the positions and angles of multiple human body parts to be measured, and ground reaction forces are necessary for some kinetic indices. Therefore, the measurement of kinetic indices requires laboratory settings. The margin of stability (MoS) [9]–[11], feasible

stability region [12], and centroidal momentum [13]¹ are examples of kinetic gait stability indices. Meanwhile, kinematic indices are typically computed using kinematic information from few body parts, which can be easily acquired through inertial measurements. However, kinematic indices may not be directly related to kinetic stability indices [6], [12], [14]–[16]. For example, the maximum Lyapunov exponent [17], [18], maximum Floquet multiplier [19], and harmonic ratios [20], [21] are popular kinematic indices.

Kinematic stability indices can be invaluable for clinical and commercial applications [22], [23] because of their relative ease of measurement outside laboratory environments; hence, many studies have compared kinetic and kinematic indices. For example, the short-term Lyapunov exponents and minimum MoS values in the anterior and mediolateral

The associate editor coordinating the review of this manuscript and approving it for publication was Kang Li.

¹This index is often applied to bipedal robots.

directions were found to exhibit different properties [6], [14] and do not exhibit substantial correlation [15]. In another study [12], several kinetic and kinematic indices including the MoS and Lyapunov exponent were compared to predict falls, and it was concluded that these indices exhibited distinct properties. In previous approaches, major kinetic and kinematic indices were compared. However, we will employ a different approach by constructing a novel kinematic index that exhibits a correlation with a major kinetic stability index. One objective of this study is to find to what extent the value of a kinetic stability index based on force information including ground reaction forces can be estimated from motion information including the velocities of body segments. Kinematic indices can be a partial substitute for kinetic indices because kinematics and kinetics are physically consistent with each other.

We utilize the MoS as a referential kinetic index and establish a novel kinematic stability index such that the kinetic and kinematic indices exhibit a correlation. This kinematic index is based on the time-series of triaxial velocities at the center of gravity of a human body. To construct the proposed index, a partial least squares (PLS) regression [24] is used to compute the principal motion analysis (PMA) [25]–[27]. The PMA decomposes a sample of a multivariate time-series into several principal motions (which are independent multivariate time-series) to construct a gait motion. In the case of normal gait, two to three types of principal motions largely represent the variations of the motion sample set [25], [27], [28]. The combination of PLS and PMA enables us to compute principal motions whose scores exhibit a correlation with the MoS values and their meaning can be interpreted by reviewing the principal motions. In our previous work, we applied this method to the MoS in the forward direction for a small sample of 20 people [29]. In this study, we constructed a kinematic gait stability index that correlated with the MoS in the mediolateral direction and enhanced the validity of the index by using the gait data of 60 elderly subjects and a cross-validation method. The number of participants and cross-validation are important aspects to investigate the generality of the new stability index. Further, the principal motions were compared with representative gait parameters to validate their meanings.

II. KINETIC GAIT STABILITY INDEX: MARGIN OF STABILITY

The MoS [9] is a major kinetic index for gait stability with good validity [7], [31] and experimental demonstration [32]. A larger MoS value indicates a greater resistance to falls during normal walking. In the present study, we evaluated the MoS values along the mediolateral direction of participants on the basis of the extrapolation of the center of mass (XCoM) [9]. As shown in Fig. 1 (a), the human body was regarded as an inverted pendulum with a constant leg length l in a coordinate space defined by the x -axis (right for positive), y -axis (anterior for positive), and z -axis (upward for positive). The coordinate vector of XCoM (x_{com}) indicates the limits

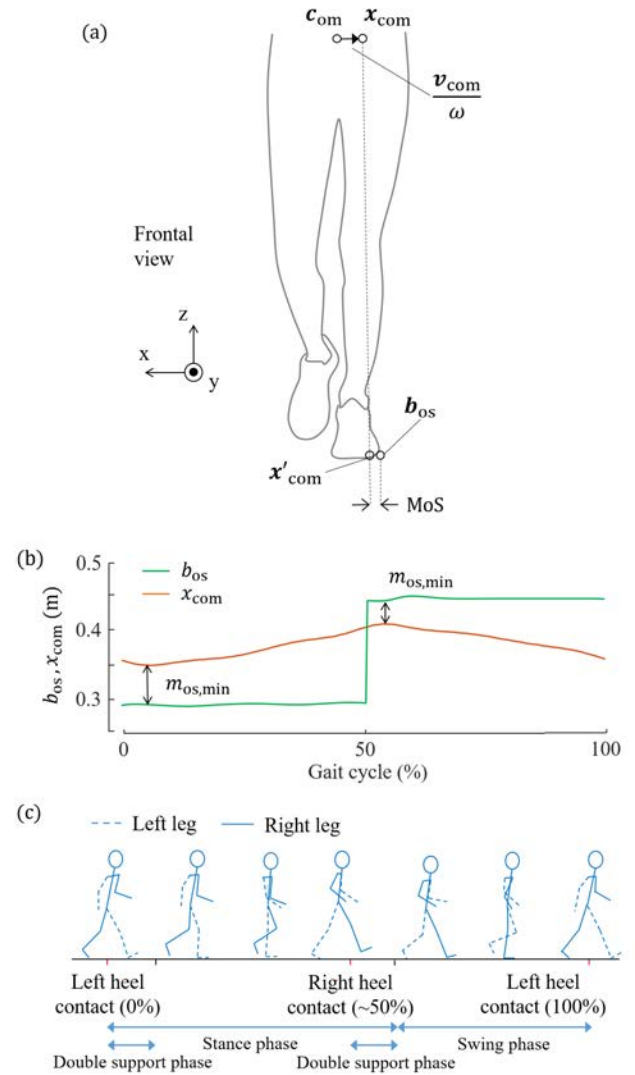


FIGURE 1. Margin of stability (MoS) value and 100% gait cycle. (a) Definition of the mediolateral MoS. x'_{com} is the point corresponding to x_{com} on the ground. b_{os} is the coordinate of the support base edge. m_{os} is computed using b_{os} and x'_{com} . (b) Example of the variations in the base of stability and center of mass in the x -direction (b_{os} , x_{com}). The smallest MoS value can be observed at approximately $\sim 10\%$ and $\sim 60\%$ of the gait cycle. (c) Gait cycle starting from the left-heel contact (0%) and ending at the following left-heel contact (100%). Modified from [30].

of the center of mass (CoM) movement at each moment. If the XCoM is outside the end of the base of support (BoS), a fall will be induced unless a new leading foot touches the ground. Since the MoS indicates walking stability at each instant, it is also used for evaluating perturbation responses during walking [33], [34] and walking stability in people with musculoskeletal abnormalities [35], [36].

The position and velocity vectors of the CoM at any given moment are c_{om} and v_{com} , respectively. x_{com} is then defined as

$$x_{com} = c_{om} + \frac{v_{com}}{\omega}, \quad (1)$$

where ω is the natural frequency of the pendulum. Here, ω is calculated as

$$\omega = \sqrt{\frac{g}{l}}, \quad (2)$$

where g is the gravitational acceleration and l is the distance from the floor to the CoM in an upright posture from [6]. Details of the determination of the CoM position are described in Section III. As \mathbf{x}'_{com} is the point corresponding to \mathbf{x}_{com} on the ground, the MoS (\mathbf{m}_{os}) is the distance vector between the end of the BoS (\mathbf{b}_{os}) and \mathbf{x}'_{com} :

$$\mathbf{m}_{os} = \mathbf{b}_{os} - \mathbf{x}'_{com}. \quad (3)$$

Following earlier studies [6], [9]–[11], we use the minimum absolute value of \mathbf{m}_{os} within the period of a gait cycle as the stability index. The minimum MoS is observed during the double support phases at approximately 10% or 60% of the gait cycle, as shown in Fig. 1 (b).

III. ANALYSIS OF GAIT MOTIONS

We analyzed a database of gait motion [38]. The analyzed data included 60 elderly adults (mean age: 67.6 ± 3.4 (standard deviation) years; height: 159.6 ± 7.6 cm; weight: 60.6 ± 9.3 kg) without any gait-related abnormalities declared. Participants walked on a 10 m line, and their two steps near the center of the course were used for the analysis described below. The comfortable gait speed was selected, and five trials were analyzed per participant. The whole-body motion of the participants was measured using a camera-based motion capture system with a sampling frequency of 200 Hz. A Butterworth low-pass filter with a cutoff frequency of 6 Hz was applied to the marker positions. The measurement details are elaborated in [38].

We defined a gait cycle as the steps starting from left-heel contact to the next left-heel contact, as shown in Fig. 1 (c). We analyzed three axial CoM velocities, which were computed by differentiating the CoM position for each axis. The CoM position was defined as the center of the sacral spine and the two anterior superior iliac spines.

We calculated various gait parameters to understand the physical meanings of the principal motions that were obtained. The definitions of each gait parameter are presented in Table 1. Note that these gait parameters are not necessary to compute the kinematic index; however, they were used to discuss the validity of the kinematic index established in the present study. The parameters were calculated by using software built in [37].

IV. GAIT STABILITY INDEX BASED ON KINEMATIC INFORMATION

We established a kinematic gait stability index that correlates with the kinetic gait stability index (MoS) using the time series of three axial CoM velocities. For this purpose, we adapted PLS [24] to PMA. In PMA, each gait motion is approximated using a linear summation of several principal motions, whereas PLS is a supervised multivariate analysis

method that extends PMA to find the principal motions whose scores (such as magnitudes) exhibit correlations with the MoS. The new kinematic stability index is then defined using a linear summation of several principal motion scores.

Each axial component of the CoM velocities was discretized every 1% of the gait cycle and then normalized (z -score) among all trials. The minimum MoS values were also normalized among all trials. The samples whose normalized minimum MoS values were greater than 2.58 or smaller than -2.58 were excluded as outliers. At the k -th trial ($k \in \{1, \dots, k'\}$) for direction $j \in \{x, y, z\}$, the time-series vector of the CoM velocity $\mathbf{v}_{com,j,k} \in \mathbb{R}^{101 \times 1}$ was defined as comprising 101 discretized instances (one value for each percentage of the gait cycle):

$$\mathbf{v}_{com,j,k} = (v_{com,j,k,1}, v_{com,j,k,2}, \dots, v_{com,j,k,101})^T. \quad (4)$$

Using this vector, a column vector $\mathbf{b}_k \in \mathbb{R}^{303 \times 1}$ is extended as follows:

$$\mathbf{b}_k = (v_{com,x,k}^T, v_{com,y,k}^T, v_{com,z,k}^T)^T. \quad (5)$$

The discrete time-series of all of the gait motions are expressed by the matrix $\mathbf{B} \in \mathbb{R}^{k' \times 303}$ as follows:

$$\mathbf{B} = (\mathbf{b}_1, \dots, \mathbf{b}_k, \dots, \mathbf{b}_{k'})^T, \quad (6)$$

where k' is the number of gait samples. $k' = 291$ (60 participants \times 5 trials $-$ 9 outliers) in this study.

The procedure of the PLS is now shown. The model formulas of the PLS are

$$\mathbf{B} = \sum_{l=1}^s \mathbf{t}_l \mathbf{p}_l^T + \mathbf{E} \quad (7)$$

and

$$\mathbf{m}_{os,min} = \sum_{l=1}^s q_l \mathbf{t}_l + \mathbf{e}. \quad (8)$$

Here, $\mathbf{m}_{os,min} \in \mathbb{R}^{k' \times 1}$ stores the minimum MoS values computed from each of the k' trials. s is the number of principal motions, $\mathbf{t}_l \in \mathbb{R}^{k' \times 1}$ is the score of all samples for the l -th principal motion, $\mathbf{p}_l \in \mathbb{R}^{303 \times 1}$ is the load of the l -th principal motion, q_l is the coefficient for the scores of the l -th principal motion, and \mathbf{E} and \mathbf{e} are the regression errors of \mathbf{B} and $\mathbf{m}_{os,min}$, respectively. Based on these formulas, we determined \mathbf{t}_1 such that the covariance with $\mathbf{m}_{os,min}$ is maximized:

$$\mathbf{t}_1 = \mathbf{B} \left(\frac{\mathbf{B}^T \mathbf{m}_{os,min}}{\|\mathbf{B}^T \mathbf{m}_{os,min}\|} \right). \quad (9)$$

Here, $\|\cdot\|$ represents the L^2 norm. \mathbf{p}_1 and q_1 are determined such that the sum of the squares of the elements of \mathbf{E} and \mathbf{e} are minimized, respectively.

$$\mathbf{p}_1 = \frac{\mathbf{B}^T \mathbf{t}_1}{\mathbf{t}_1^T \mathbf{t}_1} \quad (10)$$

$$q_1 = \frac{\mathbf{m}_{os,min}^T \mathbf{t}_1}{\mathbf{t}_1^T \mathbf{t}_1} \quad (11)$$

TABLE 1. Definition of the gait parameters modified from [37]. The joint angles were determined at each instance of the toe-off and heel-contact. These gait parameters were computed to interpret the principal motions. CoM refers to center of mass.

Right step length	Distance in the forward direction from the left-heel contact position to the next right-heel contact position. The heel position was defined by a marker attached to the heel.
Left step length	Distance in the forward direction from the right-heel contact position to the following left-heel contact position
Stride length	Sum of the right and left step lengths
Step width	Distance in the lateral direction between heel contact positions of both legs
Minimum foot clearance	Distance from the sole of the foot to the floor when the sole of the swinging leg is horizontal. The sole was defined by heel and toe markers. The height of the sole was adjusted to match the ground level at the upright posture.
Kick-up angle	Angle of the sole of the foot to the floor at the instance of toe-off.
Percentage of the CoM position (lateral)	Percentage of the lateral distance from the CoM to the left-heel position to the step width at the instance of right heel-contact.
Percentage of the CoM position (forward)	Percentage of the anteroposterior distance from the CoM to the left-heel position to the step length at the instance of right heel-contact.
Upper body angle	Pitch angle of the line connecting the midpoint between C7 and the upper sternal margin, and the midpoint between the fenestra and T10 (behind the fenestra) relative to the vertical line or gravity direction.
Thigh flexion angle	Angle between line α , which connects the greater trochanter and knee joint, and the vertical line. Positive for hip flexion. The knee joint was defined as the center of the lateral and medial condyles of the femur.
Knee extension angle	Angle between lines α and β connecting the knee and ankle joints. The ankle joint was defined as the center of the lateral and medial malleoli.
Lower thigh extension angle	Angle between line β and vertical line. Positive for knee extension.

Next, we determined the scores of the second principal motions t_2 , such that the covariance with $m_{os,min} - q_1 t_1$ is maximized. For this computation, matrix B and $m_{os,min}$ are updated as follows:

$$m_{os,min,2} = m_{os,min} - q_1 t_1, \quad (12)$$

$$B_2 = B - t_1 p_1^T. \quad (13)$$

Then, following (9)–(11), t_2, p_2 and q_2 are computed by using B_2 and $m_{os,min,2}$. In general, the l -th principal motion vector p_l and corresponding score vector t_l are computed by using

$$m_{os,min,l} = m_{os,min} - \sum_{u=1}^{l-1} q_u t_u, \quad (14)$$

$$B_l = B - \sum_{u=1}^{l-1} t_u p_u^T. \quad (15)$$

This process was repeated to compute the third and successive principal motions.

Using the s principal motions, $m_{os,min}$ was predicted as

$$\hat{m}_{os,min} = \sum_{l=1}^s q_l t_l. \quad (16)$$

We determined s on the basis of the two-fold cross validation such that the correlation between the observed and estimated $m_{os,min}$ became maximized. For this, the sixty participants were randomly divided into two groups: learning and testing. Each group included 15 males and 15 females.

V. RESULTS

Table 2 (a) shows the correlation coefficients between the scores of the first to fifth principal motions and the minimum MoS. The correlation coefficients ranged from 0.58 to 0.10. Table 2 (b) shows the results of the two-fold cross-validation.

TABLE 2. (a) Correlation coefficients between the principal motion scores and minimum MoS values in the lateral direction. ** and *** represent a statistical significance at $p < 0.01$ and $p < 0.001$, respectively. (b) Correlation coefficient between the estimated and observed minimum MoS values by 2-fold cross-validation. All participants were randomly classified into two groups. When the training data were group 1, those for group 2 were tested and vice versa.

(a)	Minimum MoS	
	1st principal motion	0.58***
2nd principal motion	0.22***	
3rd principal motion	0.28***	
4th principal motion	0.15**	
5th principal motion	0.10	

(b)	Number of principal motions	Training data		Mean
		Group 1	Group 2	
	1	0.38	0.41	0.40***
	2	0.41	0.47	0.44***
	3	0.57	0.53	0.55***
	4	0.46	0.48	0.47***
	5	0.40	0.34	0.37***

These values are the correlations between the observed and estimated MoS values. The MoS was estimated as a linear sum of the scores based on the multiple principal motions computed from the learning group. The correlation between the estimated and observed MoS was the largest when the three principal motions were included in the analysis. Therefore, we decided to use motions up until the third principal motion ($s = 3$).

The estimated MoS for the 60 participants was calculated using the linear combination of the three principal motions:

$$\hat{m}_{os,min} = 0.09t_1 + 0.02t_2 + 0.10t_3. \quad (17)$$

Fig. 2 shows a scatter plot of the estimated and observed values of the minimum MoS. The correlation coefficient was 0.68 ($t(289) = 15.77, p < 0.001$, two-tailed t -test),

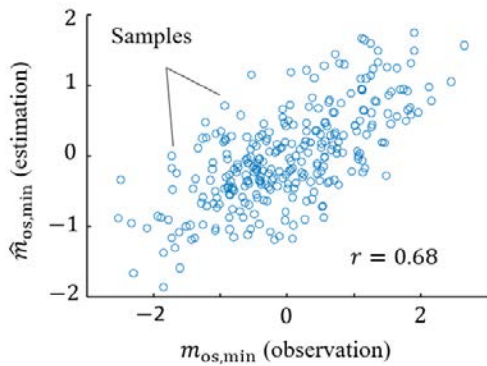


FIGURE 2. Scatter plot of minimum normalized MoS values (horizontal) and their estimation using principal motions (vertical).

indicating that our index correlates with the minimum value of the MoS.

VI. DISCUSSION

A. SEMANTIC VALIDITY OF PRINCIPAL MOTIONS

As described in Section V, the new kinematic index shows concurrent validity regarding the correlation coefficient with the minimum MoS, but the semantic validity of this index is also important. The validity of the measurement index is discussed from multiple viewpoints, including the concurrent and content validity [39]. Regarding the content validity, semantic aspects of the index are discussed. In this section, we interpret and discuss the meanings of the time-series characteristics of the principal motions and discuss their validity. Fig. 3 (a) shows the mean time-series variation of the CoM velocity. Figs. 3 (b)–(d) show the content of the first to third principal motion vectors. When the value of the principal motion is zero at a moment, the CoM velocity is the mean value among all samples due to the normalization. A positive value for the principal motion indicates that the CoM velocity is larger than the mean value. Table 3 shows the correlation coefficients between the principal motion scores and gait parameters, and these can be used to interpret the principal motion.

1) FIRST PRINCIPAL MOTION

For the first principal motion, Fig. 3 (b) shows that the velocity in the x -axis is large (positive) from the middle of the right swinging phase to the right stance phase (30%–80% of the gait cycle), and small (negative) from the middle of the left swinging phase to the left stance phase (80%–30%). This is in the same phase as the average CoM motion. According to Table 3, the scores of the first principal motion and the step width are positively correlated ($r = 0.43$) indicating that a gait with a large step width involves a greater mediolateral CoM motion.

In the y -axis, the velocity was large (positive) during the entire gait cycle, indicating a fast gait. Table 3 shows that the first principal motion scores are positively correlated

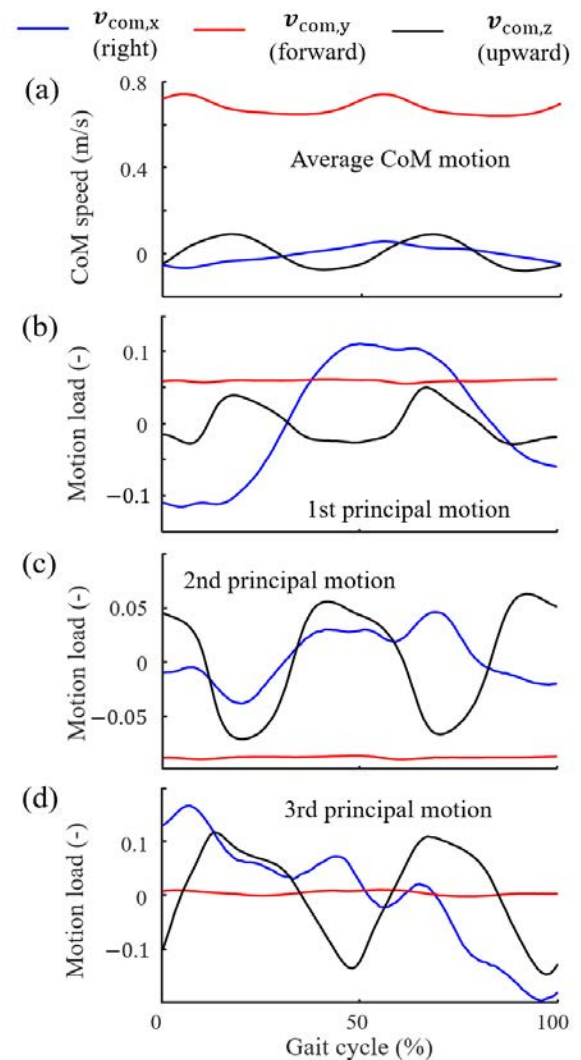


FIGURE 3. Mean center of motion (CoM) velocity and obtained principal motions. (a) Mean CoM velocity. (b)–(d) Substance of each principal motion. (b) 1st principal motion. (c) 2nd principal motion. (d) 3rd principal motion. A positive or negative load value at a moment means that the velocity is larger or smaller than the mean velocity in all trials, respectively.

with the step width and length, gait speed, and CoM position in the forward direction, and negatively correlated with the cadence and upper body pitch angle. A gait with a large first principal motion score can be a fast walking motion with a large step width and length, small cadence, and forward lean of the upper body.

The positive correlation between the first principal motion scores and minimum MoS indicates that the gait is the most stable in terms of the MoS if the gait is performed as described above. It is natural that a larger step width will result in a larger fall margin in the lateral direction. However, it is unclear whether other gait parameters, such as the upper body angle and gait speed, directly affect the MoS. In terms of the effect of the gait speed on the lateral MoS, earlier studies are not fully consistent [6], [11], [40], [41].

TABLE 3. Correlation coefficients between the principal motion scores and gait parameters. Only significant values ($p < 0.05$) are shown. PM: principal motion, CoM: center of mass, HC: heel contact, TO: toe off.

	1st PM	2nd PM	3rd PM
Right step length		-0.24	0.19
Left step length	0.14	-0.29	0.18
Stride length	0.13	-0.28	0.19
Step width	0.43		
Gait speed	0.43	-0.81	
Cadence	-0.44	0.76	
Minimum foot clearance	0.14		0.17
Kick up angle		-0.17	0.23
CoM position (lateral)			
CoM position (forward)	0.34		
Upper body angle	-0.42		
Left thigh angle (HC)		-0.36	
Left knee angle (HC)		0.18	
Left lower thigh angle (HC)	-0.14	-0.19	
Left thigh angle (TO)			
Left knee angle (TO)			-0.17
Left lower thigh angle (TO)		0.20	-0.25

For example, Alamoudi *et al.* [11] and Gill *et al.* [40] reported positive correlation coefficients between the gait speed and lateral MoS, whereas little correlation was found in [6], [41]. Caderby *et al.* [41] thought that the increase in step width associated with an increase in gait speed is a posture adjustment to remain the lateral MoS. Following this idea, the increase in step width and not in gait speed directly influences the lateral MoS. The step width may become greater at gait speeds higher than those preferred by individuals [42].

2) SECOND PRINCIPAL MOTION

Fig. 3 (c), which displays the second principal motion, shows that the velocity in the y -axis was small (negative) for the entire gait cycle. However, the CoM velocity in the z -axis was at its minimum at toe-off ($\sim 15\%$ and $\sim 65\%$ of the gait cycle) and maximum before heel contact ($\sim 40\%$ and $\sim 90\%$ of the gait cycle), which is the opposite of a normal CoM motion. The second principal motion canceled a change in the velocity in the vertical direction.

According to Table 3, the second principal motion scores were negatively correlated with step length and walking speed, and positively correlated with cadence. The second principal motion can be interpreted as a slow motion with a large cadence and small step. Joint angles such the thigh angles at heel-contact and toe-off also present the features of small steps. When the step length is small, the CoM movement in the lateral direction is small [41], [42]. In such cases, XCoM and CoM are relatively similar, and the MoS is large. Therefore, the gait motions with large scores for the second principal motion exhibit reasonably large MoS values.

Interestingly, the correlation between the principal motion scores and gait speed, and the scores and cadence, were opposite in the first and second principal motions. For the first principal motion, the scores exhibited a positive correlation coefficient with the gait speed, and faster walking was more stable than slower. As discussed above, greater step widths accompanied by greater speeds may contribute to the increase

in the mediolateral MoS. In contrast, for the second principal motion, the scores exhibited a negative correlation coefficient with the gait speed, and slower walking was more stable than faster. Gait samples with large scores of the second principal motion involve greater cadences and small stride lengths that may contribute to increase in the MoS. Earlier studies [6], [11] also reported that gaits with high cadences tend to exhibit large mediolateral MoS. If only the relationship between the gait speed and mediolateral MoS is considered, the two principal motions contradict each other. Note that older people tend to adopt large step widths and small stride lengths for lateral stabilization, which is a combination of the first and second principal motions [43].

3) THIRD PRINCIPAL MOTION

Fig. 3 (d) shows the loads of the third principal motion. In the first half of the gait cycle (0% – 60%), the velocity along the x -axis is positive, while in the second half it is negative. This profile corresponds to the differential curve of the average x -velocity, as shown in Fig. 3 (a). The large score of the third principal motion leads to the forward phase of the x -velocity.

The z -velocity is at its maximum at the instance of toe-off and minimum around the instance of heel-contact, which is close to the characteristics of the average motion of the z -velocity. This indicates a large CoM motion along the vertical direction and large step lengths.

As listed in Table 3, the scores of the third principal motion exhibit positive correlation coefficients with the step lengths, kick-up angles, and minimum foot clearance. Furthermore, a negative correlation was exhibited with the lower thigh angle at the instance of toe-off. These correlations indicate that the motions with large third principal motion scores involve an intense kick at the instance of toe-off and large step lengths. However, it is difficult to explain how these characteristics pertain to the MoS values.

B. LIMITATIONS OF THE STUDY

Here, we address the limitations and concerns of the present study. As mentioned in Section I, many representative gait stability indices do not substantially correlate with each other [6], [12], [14]–[16], [44]–[47]. This is because each index evaluates a different aspect of gait. However, the index based on the principal motion score showed a moderate correlation with the MoS, possibly because both indices are based on the CoM velocity. PMA and PLS can be applied to the time-series of other body parts. It remains to be investigated which body part's velocity or acceleration information is best in terms of the correlation with MoS. Further, it would be possible to increase the correlation between the MoS and kinematic index based on the principal motions by employing the velocities of multiple body segments. Although it is understandable how the first and second principal motions may increase the MoS values, it should be noted that the characteristics of the principal motions are only correlated with the MoS values and are not necessarily causally related.

We estimated the position of the CoM from the marker positions measured using a motion capture system and differentiated it to obtain the CoM velocity. If we use the CoM velocity measured by an inertial measurement unit, we may not be able to obtain the same results that were obtained in this study because of the influence of the sampling rate and the integration of the error. Our method should be tested using inertial measurement units because methods to assess gait stability and performance using these units are currently popular, as indicated by previous studies [16], [45], [48]–[51], and have promising accessibility.

Additionally, fall risks or abnormal walking may be more related to gait variability than to mean gait features [8], [22], [52]–[55]. For example, the variability of minimum foot clearance may be used to differentiate between those with and without trip-related histories [54] and the variability of step width can be related to fall history [55]. Our proposed method is not for evaluating the variability of gait patterns; instead, it evaluates the stability of individual strides.

The gait database we used in the present study [38] included only healthy participants. To determine the clinical validity of the kinematic index developed in this study, it is important to test individuals with a history of falls and those deemed at risk by clinical experts. Finding or establishing stability indices that can accurately estimate fall risks is a primary concern among the researchers.

VII. CONCLUSION

We developed a novel kinematic gait stability index that is consistent with the MoS in the lateral direction. Many earlier studies reported that no substantial correlation existed between currently used kinetic and kinematic gait stability indices. We applied PLS to PMA and statistically constructed an index that was correlated with the minimum value of the MoS using time-series data of the CoM velocity. Based on the three principal motions, the constructed index showed a moderate correlation coefficient of 0.68 with the MoS. Although this correlation coefficient is not very high, it can be further improved by involving the kinematic information of multiple body segments, among other methods. Furthermore, part of the principal motions can be reasonably linked with the fall margin. These results suggest that this gait stability index can be an easy-to-access alternative to the MoS.

REFERENCES

- [1] J. S. Brach, J. E. Berlin, J. M. Van Swearingen, A. B. Newman, and S. A. Studenski, "Too much or too little step width variability is associated with a fall history in older persons who walk at or near normal gait speed," *J. Neuroeng. Rehabil.*, vol. 2, p. 21, Jul. 2005.
- [2] T. M. Owings and M. D. Grabiner, "Variability of step kinematics in young and older adults," *Gait Posture*, vol. 20, no. 1, pp. 26–29, Aug. 2004.
- [3] S. A. England and K. P. Granata, "The influence of gait speed on local dynamic stability of walking," *Gait Posture*, vol. 25, no. 2, pp. 172–178, Feb. 2007.
- [4] S. M. Bruijn, J. H. van Dieën, O. G. Meijer, and P. J. Beek, "Is slow walking more stable?" *J. Biomech.*, vol. 42, no. 10, pp. 1506–1512, Jul. 2009.
- [5] D. D. Espy, F. Yang, T. Bhatt, and Y.-C. Pai, "Independent influence of gait speed and step length on stability and fall risk," *Gait Posture*, vol. 32, no. 3, pp. 378–382, Jul. 2010.
- [6] L. Hak, H. Houdijk, P. J. Beek, and J. H. van Dieën, "Steps to take to enhance gait stability: The effect of stride frequency, stride length, and walking speed on local dynamic stability and margins of stability," *PLoS ONE*, vol. 8, no. 12, Dec. 2013, Art. no. e82842.
- [7] S. M. Bruijn, O. G. Meijer, P. J. Beek, and J. H. van Dieën, "Assessing the stability of human locomotion: A review of current measures," *J. Roy. Soc., Interface*, vol. 10, no. 83, 2013, Art. no. 20120999.
- [8] D. Hamacher, N. B. Singh, J. H. Van Dieën, M. O. Heller, and W. R. Taylor, "Kinematic measures for assessing gait stability in elderly individuals: A systematic review," *J. Roy. Soc. Interface*, vol. 8, no. 65, pp. 1682–1698, Dec. 2011.
- [9] A. L. Hof, M. G. J. Gazendam, and W. E. Sinke, "The condition for dynamic stability," *J. Biomech.*, vol. 38, no. 1, pp. 1–8, 2005.
- [10] A. Hallemans, E. Verbecque, R. Dumas, L. Cheze, A. Van Hamme, and T. Robert, "Developmental changes in spatial margin of stability in typically developing children relate to the mechanics of gait," *Gait Posture*, vol. 63, pp. 33–38, Jun. 2018.
- [11] R. Alamoudi and M. Alamoudi, "Development of linear regression models to estimate the margin of stability based on spatio-temporal gait parameters," *IEEE Access*, vol. 8, pp. 19853–19859, 2020.
- [12] F. Yang and Y.-C. Pai, "Can stability really predict an impending slip-related fall among older adults?" *J. Biomech.*, vol. 47, no. 16, pp. 3876–3881, Dec. 2014.
- [13] D. E. Orin, A. Goswami, and S.-H. Lee, "Centroidal dynamics of a humanoid robot," *Auton. Robot.*, vol. 35, nos. 2–3, pp. 161–176, 2013.
- [14] L. Hak, H. Houdijk, F. Steenbrink, A. Mert, P. van der Wurff, P. J. Beek, and J. H. van Dieën, "Speeding up or slowing down: Gait adaptations to preserve gait stability in response to balance perturbations," *Gait Posture*, vol. 36, no. 2, pp. 260–264, Jun. 2012.
- [15] M. F. Vieira, G. S. de Sá e Souza, G. C. Lehen, F. B. Rodrigues, and A. O. Andrade, "Effects of general fatigue induced by incremental maximal exercise test on gait stability and variability of healthy young subjects," *J. Electromyogr. Kinesiol.*, vol. 30, pp. 161–167, Oct. 2016.
- [16] K. Kazumura, Y. Akiyama, T. Naganeo, S. Okamoto, and Y. Yamada, "Index of gait stability using inertial measurement unit," in *Proc. IEEE 3rd Global Conf. Life Sci. Technol. (LifeTech)*, Mar. 2021, pp. 29–30.
- [17] J. B. Dingwell and J. P. Cusumano, "Nonlinear time series analysis of normal and pathological human walking," *Chaos*, vol. 10, no. 4, pp. 848–863, Dec. 2000.
- [18] S. Kim, D. Srinivasan, M. A. Nussbaum, and A. Leonessa, "Human gait during level walking with an occupational whole-body powered exoskeleton: Not yet a walk in the park," *IEEE Access*, vol. 9, pp. 47901–47911, 2021.
- [19] J. B. Dingwell, H. G. Kang, and L. C. Marin, "The effects of sensory loss and walking speed on the orbital dynamic stability of human walking," *J. Biomech.*, vol. 40, no. 8, pp. 1723–1730, Jan. 2007.
- [20] G. L. Smidt, J. S. Arora, and R. C. Johnston, "Accelerographic analysis of several types of walking," *Amer. J. Phys. Med.*, vol. 50, no. 6, pp. 285–300, Dec. 1971.
- [21] H. J. Yack and R. C. Berger, "Dynamic stability in the elderly: Identifying a possible measure," *J. Gerontol.*, vol. 48, no. 5, pp. M225–M230, Sep. 1993.
- [22] Y. Yan, O. M. Omisore, Y. Xue, H. Li, Q. Liu, Z. Nie, J. Fan, and L. Wang, "Classification of neurodegenerative diseases via topological motion analysis—A comparison study for multiple gait fluctuations," *IEEE Access*, vol. 8, pp. 96363–96377, 2020.
- [23] K. Jun, Y. Lee, S. Lee, D.-W. Lee, and M. S. Kim, "Pathological gait classification using Kinect v2 and gated recurrent neural networks," *IEEE Access*, vol. 8, pp. 139881–139891, 2020.
- [24] S. Wold, M. Sjöström, and L. Eriksson, "PLS-regression: A basic tool of chemometrics," *Chemometrics Intell. Lab. Syst.*, vol. 58, no. 2, pp. 109–130, 2001.
- [25] F. C. Park and K. Jo, "Movement primitives and principal component analysis," in *On Advances in Robot Kinematics*. Berlin, Germany: Springer, 2004, pp. 97–106.
- [26] N. Yamada, S. Okamoto, Y. Akiyama, and Y. Yamada, "Principal motion analysis of manual stretching techniques for the ankle joints," *J. Phys. Therapy Sci.*, vol. 32, no. 9, pp. 584–590, 2020.
- [27] T. Iwasaki, S. Okamoto, Y. Akiyama, and Y. Yamada, "Principal motion ellipsoids: Gait variability index invariant with gait speed," *IEEE Access*, vol. 8, pp. 213330–213339, 2020.
- [28] H. Oshima, S. Aoi, T. Funato, N. Tsujiuchi, and K. Tsuchiya, "Variant and invariant spatiotemporal structures in kinematic coordination to regulate speed during walking and running," *Frontiers Comput. Neurosci.*, vol. 13, p. 63, Sep. 2019.

- [29] T. Iwasaki, S. Okamoto, Y. Akiyama, T. Inagaki, and Y. Yamada, "Kinematic gait stability index highly correlated with the margin of stability: Concept and interim report," in *Proc. IEEE/SICE Int. Symp. Syst. Integr. (SII)*, Jan. 2021, pp. 347–350.
- [30] T. Iwasaki, S. Okamoto, Y. Akiyama, and Y. Yamada, "Principal motion ellipsoids: Gait variability index based on principal motion analysis," in *Proc. IEEE/SICE Int. Symp. Syst. Integr. (SII)*, Jan. 2020, pp. 489–494.
- [31] *Balance Augmentation in Locomotion, Through Anticipative, Natural and Cooperative Control of Exoskeletons*, Report of BALANCE-Deliverable 3.1-Stability Index, Fundacion Tecnalia Res. Innov., Derio, Spain, 2014.
- [32] H. Vallery, A. Bögel, C. C. O'Brien, and R. Riener, "Cooperative control design for robot-assisted balance during gait," *Automatisierungstechnik*, vol. 60, no. 11, pp. 715–720, 2012.
- [33] A. Hof, S. Vermerris, and W. Gjaltema, "Balance responses to lateral perturbations in human treadmill walking," *J. Exp. Biol.*, vol. 213, no. 15, pp. 2655–2664, 2010.
- [34] P. M. M. Young, J. M. Wilken, and J. B. Dingwell, "Dynamic margins of stability during human walking in destabilizing environments," *J. Biomech.*, vol. 45, no. 6, pp. 1053–1059, 2012.
- [35] A. L. Hof, R. M. van Bockel, T. Schoppen, and K. Postema, "Control of lateral balance in walking: Experimental findings in normal subjects and above-knee amputees," *Gait Posture*, vol. 25, no. 2, pp. 250–258, 2007.
- [36] R. Rethwilm, H. Böhm, M. Haase, D. Perchthaler, C. U. Dussa, and P. Federolf, "Dynamic stability in cerebral palsy during walking and running: Predictors and regulation strategies," *Gait Posture*, vol. 84, pp. 329–334, Feb. 2021.
- [37] T. Mayumi, Y. Akiyama, S. Okamoto, and Y. Yamada, "Identification of healthy elderly's gait characteristics by analyzing gait parameters," in *Proc. IEEE Int. Conf. Intell. Saf. Robot. (ISR)*, Mar. 2021, pp. 220–223.
- [38] Y. Kobayashi, N. Hida, K. Nakajima, M. Fujimoto, and M. Mochimaru, "2019: AIST gait database," Nat. Inst. Adv. Ind. Sci. Technol., Tsukuba, Japan, Tech. Rep., 2019.
- [39] *Standards for Educational and Psychological Testing*, Amer. Psychol. Assoc., Nat. Council Meas. Educ., Amer. Educ. Res. Assoc., Washington, DC, USA, 2014.
- [40] L. Gill, A. H. Huntley, and A. Mansfield, "Does the margin of stability measure predict medio-lateral stability of gait with a constrained-width base of support?" *J. Biomech.*, vol. 95, Oct. 2019, Art. no. 109317.
- [41] T. Caderby, E. Yiu, N. Peyrot, M. Begon, and G. Dalleau, "Influence of gait speed on the control of mediolateral dynamic stability during gait initiation," *J. Biomech.*, vol. 47, no. 2, pp. 417–423, Jan. 2014.
- [42] J. L. Helbostad and R. Moe-Nilssen, "The effect of gait speed on lateral balance control during walking in healthy elderly," *Gait Posture*, vol. 18, no. 2, pp. 27–36, Oct. 2003.
- [43] M. A. Schragger, V. E. Kelly, R. Price, L. Ferrucci, and A. Shumway-Cook, "The effects of age on medio-lateral stability during normal and narrow base walking," *Gait Posture*, vol. 28, no. 3, pp. 466–471, Oct. 2008.
- [44] T. Inagaki, Y. Akiyama, S. Okamoto, T. Iwasaki, and Y. Yamada, "Relationship between margin of stability and maximum Lyapunov exponent during short-term walking in the elderly," in *Proc. IEEE/SICE Int. Symp. Syst. Integr.*, Jan. 2021, pp. 347–350.
- [45] F. Riva, M. C. Bisi, and R. Stagni, "Gait variability and stability measures: Minimum number of strides and within-session reliability," *Comput. Biol. Med.*, vol. 50, pp. 9–13, Jul. 2014.
- [46] P. Terrier and O. Déria, "Kinematic variability, fractal dynamics and local dynamic stability of treadmill walking," *J. Neuroeng. Rehabil.*, vol. 8, no. 1, p. 12, Dec. 2011.
- [47] J. B. Dingwell, J. P. Cusumano, P. R. Cavanagh, and D. Sternad, "Local dynamic stability versus kinematic variability of continuous overground and treadmill walking," *J. Biomech. Eng.*, vol. 123, no. 1, pp. 27–32, Feb. 2001.
- [48] H. Jebelli, C. R. Ahn, and T. L. Stentz, "Comprehensive fall-risk assessment of construction workers using inertial measurement units: Validation of the gait-stability metric to assess the fall risk of iron workers," *J. Comput. Civil Eng.*, vol. 30, no. 3, May 2016, Art. no. 04015034.
- [49] S. M. Cain, R. S. McGinnis, S. P. Davidson, R. V. Vitali, N. C. Perkins, and S. G. McLean, "Quantifying performance and effects of load carriage during a challenging balancing task using an array of wireless inertial sensors," *Gait Posture*, vol. 43, pp. 65–69, Jan. 2016.
- [50] G. Bastas, J. J. Fleck, R. A. Peters, and K. E. Zelik, "IMU-based gait analysis in lower limb prosthesis users: Comparison of step demarcation algorithms," *Gait Posture*, vol. 64, pp. 30–37, Jul. 2018.
- [51] S. Qiu, L. Liu, Z. Wang, S. Li, H. Zhao, J. Wang, J. Li, and K. Tang, "Body sensor network-based gait quality assessment for clinical decision-support via multi-sensor fusion," *IEEE Access*, vol. 7, pp. 59884–59894, 2019.
- [52] Y. Moon, J. Sung, R. An, M. E. Hernandez, and J. J. Sosnoff, "Gait variability in people with neurological disorders: A systematic review and meta-analysis," *Hum. Movement Sci.*, vol. 47, pp. 197–208, Jun. 2016.
- [53] M. E. Taylor, K. Delbaere, A. S. Mikolaizak, S. R. Lord, and J. C. T. Close, "Gait parameter risk factors for falls under simple and dual task conditions in cognitively impaired older people," *Gait Posture*, vol. 37, no. 1, pp. 126–130, Jan. 2013.
- [54] A. H. Khandoker, S. B. Taylor, C. K. Karmakar, R. K. Begg, and M. Palaniswami, "Investigating scale invariant dynamics in minimum toe clearance variability of the young and elderly during treadmill walking," *IEEE Trans. Neural Syst. Rehabil. Eng.*, vol. 16, no. 4, pp. 380–389, Aug. 2008.
- [55] J. S. Brach, J. E. Berlin, J. M. Van Swearingen, A. B. Newman, and S. A. Studenski, "Too much or too little step width variability is associated with a fall history in older persons who walk at or near normal gait speed," *J. Neuroeng. Rehabil.*, vol. 2, p. 21, Jul. 2005.



TOMOYUKI IWASAKI received the B.S. and M.S. degrees in mechanical engineering from Nagoya University, in 2019 and 2021, respectively. He is currently a Mechanical Engineer. His research interest includes human motion analysis.



SHOGO OKAMOTO (Member, IEEE) received the Ph.D. degree in information sciences from Tohoku University, in 2010. From 2010 to 2021, he was with Nagoya University as an Assistant Professor and an Associate Professor. He is currently an Associate Professor with the Department of Computer Sciences, Tokyo Metropolitan University. His research interests include haptics, assistive robotics, human-centered informatics, and affective computing.



YASUHIRO AKIYAMA (Member, IEEE) received the B.E. degree in engineering from the Tokyo Institute of Technology, Tokyo, Japan, in 2006, and the M.S. and Ph.D. degrees in engineering from The University of Tokyo, Tokyo, in 2008 and 2011, respectively. He was an Assistant Professor with the Department of Mechanical Systems, Nagoya University, until 2022. He is currently an Associate Professor with the Department of Mechanical Engineering and Robotics, Shinshu University,

Japan. His main research interests include mechanical safety, human-robot interaction, and biomechanics.



YOJI YAMADA (Member, IEEE) received the Ph.D. degree from the Tokyo Institute of Technology. Since 1983, he has been at the Toyota Technological Institute, Nagoya, Japan. In 2004, he joined the National Institute of Advanced Industrial Science and Technology, as a Leader of the Safety Intelligence Research Group. In 2009, he joined the Department of Mechanical Systems Engineering, Graduate School of Engineering, Nagoya University as a Professor.

• • •